Articles

Oxygen Activation by a Mixed-Valent, Diiron(II/III) Cluster in the Glycol Cleavage Reaction Catalyzed by *myo*-Inositol Oxygenase†

Gang Xing,‡ Eric W. Barr,‡ Yinghui Diao,‡ Lee M. Hoffart,‡ K. Sandeep Prabhu,§ Ryan J. Arner,§ C. Channa Reddy,§ Carsten Krebs,‡,|| and J. Martin Bollinger, Jr.*,‡,||

Departments of Biochemistry and Molecular Biology, Veterinary and Biomedical Sciences, and Chemistry, The Pennsylvania State University, University Park, Pennsylvania 16802

Received December 23, 2005; Revised Manuscript Received February 17, 2006

ABSTRACT: *myo*-Inositol oxygenase (MIOX) catalyzes the ring-cleaving, four-electron oxidation of its cyclohexan-(*1,2,3,4,5,6-hexa*)-ol substrate (*myo*-inositol, MI) to D-glucuronate (DG). The preceding paper [Xing, G., Hoffart, L. M., Diao, Y., Prabhu, K. S., Arner, R. J., Reddy, C. C., Krebs, C., and Bollinger, J. M., Jr. (2006) *Biochemistry 45*, 5393−5401] demonstrates by Mössbauer and electron paramagnetic resonance (EPR) spectroscopies that MIOX can contain a non-heme dinuclear iron cluster, which, in its mixed-valent (II/III) and fully oxidized (III/III) states, is perturbed by binding of MI in a manner consistent with direct coordination. In the study presented here, the redox form of the enzyme that activates O_2 has been identified. L-Cysteine, which was previously reported to accelerate turnover, reduces the fully oxidized enzyme to the mixed-valent form, and O_2, the cosubstrate, oxidizes the fully reduced form to the mixed-valent form with a stoichiometry of one per O_2. Both observations implicate the mixed-valent, diiron(II/III) form of the enzyme as the active state. Stopped-flow absorption and freeze-quench EPR data from the reaction of the substrate complex of mixed-valent MIOX [MIOX(II/III)·MI] with limiting O_2 in the presence of excess, saturating MI reveal the following cycle: (1) MIOX(II/III)·MI reacts rapidly with O_2 to generate an intermediate (**H**) with a rhombic, $g < 2$ EPR spectrum; (2) a form of the enzyme with the same absorption features as MIOX(II/III) develops as **H** decays, suggesting that turnover has occurred; and (3) the starting MIOX(II/III)·MI complex is then quantitatively regenerated. This cycle is fast enough to account for the catalytic rate. The DG/O_2 stoichiometry in the reaction, 0.8 ± 0.1, is similar to the theoretical value of 1, whereas significantly less product is formed in the corresponding reaction of the fully reduced enzyme with limiting O_2. The DG/O_2 yield in the latter reaction decreases as the enzyme concentration is increased, consistent with the hypothesis that initial conversion of the reduced enzyme to the MIOX(II/III)·MI complex and subsequent turnover by the mixed-valent form is responsible for the product in this case. The use of the mixed-valent, diiron(II/III) cluster by MIOX represents a significant departure from the mechanisms of other known diiron oxygenases, which all involve activation of O_2 from the II/II manifold.

myo-Inositol oxygenase (MIOX,[1] EC 1.13.99.1) catalyzes production of D-glucuronate (DG) from *myo*-inositol (MI) and dioxygen (eq 1) (*1*−*3*) to initiate the only known pathway in humans for catabolism of MI (*4*), the sugar backbone of cell-signaling phosphoinositides.

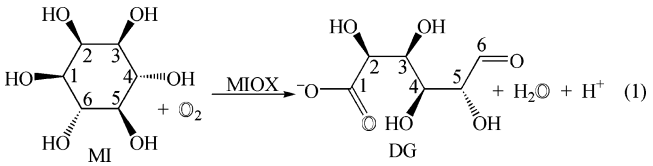

(1)

Although MIOX was first described and shown to require iron nearly 50 years ago, little insight into its structure or catalytic mechanism has subsequently emerged. The preceding paper (*5*) presents spectroscopic evidence that MIOX can support assembly of a coupled dinuclear iron cluster, suggesting that the enzyme belongs to the non-heme diiron oxygenase/oxidase family that also includes bacterial hy-

† This work was supported by an Innovative Biotechnology Seed Grant from Johnson and Johnson and The Huck Institutes for the Life Sciences at the Pennsylvania State University.

* To whom correspondence should be addressed: Department of Biochemistry and Molecular Biology, 208 Althouse Laboratory, University Park, PA 16802. Phone: (814) 863-5707. Fax: (814) 863-7024. E-mail: jmb21@psu.edu.

‡ Department of Biochemistry and Molecular Biology.

§ Department of Veterinary and Biomedical Sciences.

|| Department of Chemistry.

[1] Abbreviations: MIOX, *myo*-inositol oxygenase; MI, *myo*-inositol; DG, D-glucuronate; sMMO, soluble methane monooxygenase; RNR-R2, R2 subunit of class I ribonucleotide reductase; EPR, electron paramagnetic resonance; *m*/*z*, mass-to-charge ratio; L-Cys, L-cysteine; Asc, ascorbate; SF, stopped-flow; FQ, freeze-quench; *v*, turnover velocity; V_{max}, maximal turnover velocity.

10.1021/bi0526276 CCC: $33.50
Published on Web 04/08/2006

drocarbon hydroxylases [e.g., soluble methane monooxygenase (sMMO), toluene 4-monooxygenase, and alkane ω-hydroxylase], plant fatty acyl desaturases (e.g., stearoyl acyl carrier protein Δ^9-desaturase), and protein R2 of class I ribonucleotide reductase (RNR-R2) (*6*−*10*). The recognition that MIOX belongs to this family does not immediately reveal the mechanism of its unique reaction. The outcome, a four-electron oxidation by 1 equiv of O_2 (*2*), is distinct from the one-electron and two-electron oxidations effected by other family members and is not easily envisaged to arise via the canonical mechanism for the family (*6*−*10*). In this mechanism, O_2 reacts with the diiron(II/II) cluster to form a peroxodiiron(III/III) intermediate. Cleavage of the peroxide bond produces a high-valent [Fe_2(III/IV) or Fe_2(IV/IV)] diiron complex, which subsequently extracts electrons from the target for oxidation (the substrate or, in the case of RNR-R2, the internal tyrosine residue that is oxidized to a radical). In all cases, a diiron(III/III) "product" state of the cluster is generated as part of each O_2 activation event. For subsequent events to occur, the cofactor must be returned to the "reactant" diiron(II/II) state, with electrons provided ultimately by NAD(P)H (*6*−*10*). This cycling of the cofactor and oxidation of a nicotinamide cosubstrate ensure that at most two electrons can be extracted from the substrate. How, then, can MIOX use its diiron cluster to activate O_2 for a four-electron oxidation outcome?

In this study, we have begun to answer this question by determining which oxidation state of the diiron cluster activates O_2 for DG production. Results of single-turnover experiments suggest, surprisingly, that the mixed-valent, II/III oxidation state, rather than the conventional II/II state, is the reactive enzyme form. This finding provides an important clue regarding how the unique outcome is achieved. Moreover, the use of the mixed-valent cluster can explain previous reports that reductants such as L-cysteine (L-Cys) reactivate MIOX and accelerate catalysis in the steady state (*2*, *11*) despite the fact that the reaction is already charge-balanced without additional reducing equivalents.

MATERIALS AND METHODS

Materials. Growth medium components and biochemical reagents used in overexpression and purification of MIOX were obtained from sources listed previously (*12*). MI was obtained from Sigma (St. Louis, MO). [U-^{14}C]MI (300 Ci/mol) was purchased from American Radiolabeled Chemicals, Inc. (St. Louis, MO). It was purified by filtration through AG1-x8 anion-exchange resin (hydroxide form; Bio-Rad, Hercules, CA) to remove a contaminant that otherwise coelutes with the product in the assay procedure.

Preparation of Iron-Free MIOX. MIOX was expressed in *Escherichia coli* in the presence of the iron chelator, 1,10-phenanthroline, and purified in its iron-free form as described in the preceding paper (*5*).

O_2 Quantitation. Quantities of O_2(g) were calculated according to the ideal gas law. Determination of the solubility of O_2 in MIOX buffer [50 mM Bis-Tris-acetate (pH 6.0) and 10% (w/w) glycerol] for calculation of the O_2 concentration in reactant solutions is described in the Supporting Information.

Preparation of MIOX(II/II) and MIOX(II/II)·MI. Solutions of iron-free MIOX were rendered free of O_2 by cycles of gentle evacuation and refilling with argon, as previously described (*12*). In an anoxic chamber (MBraun) containing <1 ppm O_2, O_2-free stock solutions of Fe(II), L-ascorbate (Asc) or L-Cys (when appropriate), and MI were added to the protein. For ease of designation, it is hereafter presumed that addition of 2 equiv of Fe(II) to the iron-free protein generated the diiron(II/II) form of the enzyme, MIOX(II/II). However, we note that the spectroscopic data in the preceding paper (*5*) definitively establish the presence of a diiron cluster for only the II/III and III/III oxidation states. It is further presumed (for ease of designation) that subsequent addition of MI to 50−100 mM resulted in formation of MIOX(II/II)·MI, although binding of the substrate to the presumptive diiron(II/II) protein has likewise not yet been directly demonstrated.

Stoichiometry of MIOX(II/III)·MI Production in the Reaction of MIOX(II/II)·MI with Limiting O_2. An O_2-free solution containing 1.1 mM MIOX, 2.1 mM Fe(II), and 50 mM MI was rapidly mixed at 5 °C with an equal volume of either O_2-free buffer (the control) or air-saturated (at 5 °C) buffer (the experiment). The reaction solution was sealed inside the reaction hose, incubated at 5 °C for 3 min, taken into the anoxic chamber, transferred to an EPR tube, and frozen. EPR spectra of the experimental and control samples were acquired with a subsaturating microwave power (conditions are given in the legend of Figure 1), and the integrated intensity of the (experiment − control) difference spectrum was compared to that from a copper(II) perchlorate standard (*13*, *14*) to determine the yield of MIOX(II/III)·MI.

Preparation of MIOX(III/III). Three different samples of MIOX(III/III) were used in determination of its activity and the effect of reductants on activity and oxidation state. The sample of MIOX(III/III) described in the legend of Figure 1 of the preceding paper (*5*) was used for several activity measurements. This sample was characterized by Mössbauer spectroscopy and shown to contain >95% of the iron in the form of MIOX(III/III). A second sample was prepared by addition of 2.2 equiv of Fe(II) to an air-saturated solution of 1.2 mM iron-free MIOX and incubation at 0 °C in air for 48 h, as described in the legend of Figure 2. This sample was characterized periodically during the incubation to monitor decay of the ∼0.3 equiv of MIOX(II/III) produced upon addition of Fe(II). The absence of precipitation of Fe(III) or protein and the evolution of the absorption spectrum of the sample during the incubation to that characteristic of MIOX(III/III) were taken as evidence that the final product was MIOX(III/III). A third sample was prepared by addition of 2.0 equiv of Fe(II) to an air-saturated solution of 20 μM iron-free MIOX and subsequent concentration of the protein to 1.0 mM. This sample was characterized by EPR spectroscopy, which showed that it did not contain a detectable quantity of MIOX(II/III), and absorption spectroscopy, which showed that it had the spectrum characteristic of MIOX(III/III). This method, addition of iron to a dilute, air-saturated solution of iron-free MIOX followed by concentration of the protein, has proven to be the most reliable method for generating MIOX(III/III) in the absence of significant quantities of contaminating MIOX(II/III).

Preparation of MIIOX(II/III) and MIOX(II/III)·MI. The mixed-valent enzyme, MIOX(II/III), was prepared by a procedure hereafter termed the "O_2-diffusion method". A solution of MIOX, 2 equiv of Fe(II), and 4−5 mM Asc (or

L-Cys) in a sealed cuvette was treated in the anoxic chamber with 1−3 equiv of O_2(g), which was injected into the headspace of the cuvette. The solution was incubated at 10 °C with repeated, gentle mixing until its absorption spectrum became stable. The cuvette was opened to the nitrogen atmosphere and incubated for several minutes to allow for dispersion of any remaining O_2(g). For experiments probing MI binding, this solution was used directly. For experiments examining the reaction of MIOX(II/III)·MI with O_2, MI was then added to the desired concentration.

Stopped-Flow (SF) Absorption Experiments. The SF apparatus has been described previously (*12*). In experiments to define the kinetics of substrate binding, MIOX(II/III) was prepared by the O_2-diffusion method. This solution was mixed with an equal volume of an O_2-free solution of MI. In single-turnover experiments, MI was added to MIOX(II/III) to a concentration of 15 or 50 mM, and this solution was mixed at 5 °C with an equal volume of air-saturated (at 5 or 23 °C) buffer. Reactant concentrations after mixing are given in the appropriate figure legend. The concentration of MIOX(II/III)·MI was estimated from the absorbance changes upon addition of MI to the MIOX(II/III) solution. This intensity was compared to that seen in preparation of MIOX(II/III)·MI for the EPR experiments, in which case the MIOX(II/III)·MI concentration was determined directly by EPR spectroscopy (vide infra).

Freeze-Quench (FQ) EPR Experiments. The apparatus and procedures for preparation of FQ EPR samples have been described previously (*15*). MIOX(II/III)·MI was prepared by the O_2-diffusion method (final concentrations of 0.94 mM MIOX, 1.9 mM Fe, 3.2 mM Asc, and 100 mM MI). An aliquot was frozen in an EPR tube for determination of the concentration of MIOX(II/III)·MI in the reactant solution (0.56 mM, black spectrum in Figure 5A). The integrated intensity of the axial $g < 2$ EPR signal at a subsaturating microwave power was compared to the intensity of the spectrum of a copper(II) perchlorate standard, as previously described (*13*, *14*). The spectrum of iron-free MIOX was acquired so that the contribution of the contaminating Mn(II) that copurifies with iron-free MIOX could be subtracted. In experiments with limiting O_2 (black, red, blue, green, and purple spectra in Figure 5B), the MIOX(II/III)·MI solution was mixed at 5 °C with 0.5 equiv volume of buffer containing 0.58 mM O_2 [prepared by equal-volume mixing of air-saturated and O_2-saturated (23 °C) buffer], and the reaction solution was freeze-quenched after the desired time. For the excess-O_2 sample (orange spectrum in Figure 5B), the MIOX(II/III)·MI solution was mixed with 2 equiv volumes of O_2-saturated (5 °C) buffer (giving 0.95 mM O_2), and the reaction solution was freeze-quenched after 0.020 s. The quoted reaction time for each sample is the sum of the known transit time through the reaction hose and the estimated "quench time" (the time required for cooling to a temperature at which no further reaction occurs) of 0.015 s. Following preparation of one of the limiting-O_2 samples, the reaction solution remaining in the hose was sealed inside the hose, incubated at 5 °C for 5 min, taken back into the anoxic chamber, transferred to an EPR tube, and frozen for EPR analysis (red spectrum in Figure 5A). The EPR spectrometer has been described previously (*12*). Spectral parameters are given in the appropriate figure legend.

To obtain the kinetics of the MIOX(II/III)·MI reactant complex from the time-dependent EPR spectra, the peak-to-trough intensity of the $g_\perp$ (1.81) derivative feature was used to determine relative concentrations, and the data were scaled by the initial concentration of 0.37 mM. To obtain kinetics of the intermediate state (**H**) with the rhombic $\mathbf{g} =$ (1.92, 1.76, 1.54) EPR signal, the derivative spectra were subjected to the peak-height treatments shown in the Supporting Information (Figure S4). After scaling, the intensities of the three features as functions of time gave identical kinetics. The equation describing the concentration of species B as a function of time in an A → B → C sequence was fit to these data, and the data were then scaled to have a fit amplitude (equivalent to the initial concentration of species A) of 0.19 mM, the concentration of O_2, the limiting reactant. This scaling procedure thus incorporates the assumption that the intermediate forms by reaction of MIOX(II/III)·MI and O_2 and the approximation that the extent to which it accumulates is the same as would occur if the reaction were kinetically pseudo-first-order. Both are validated by the agreement of the kinetic simulations with the data (see Results).

Kinetic Simulations. Kinetic simulations were performed with KinTekSim (KinTek Corp., Austin, TX). The mechanism and parameters are presented in Results.

MIOX Activity Assays. The kinetics of MIOX catalysis in the steady state were defined by a liquid chromatography−mass spectrometry assay. Enzyme reactions were carried out in the standard buffer [50 mM Bis-Tris-acetate (pH 6.0) and 10% (w/w) glycerol]. An air-saturated solution (1 mL) containing 1−5 μM MIOX in the desired state, MI (50 mM in standard assays and varied from 1 to 100 mM in determination of the K_M), and, when appropriate, an activating reductant was incubated at 5 °C, and the reaction was terminated at various times by addition of 200 μL aliquots to 20 μL of 1 M HCl. Each inactivated sample was centrifuged through a Microcon YM-3 centrifugal concentrator (Millipore, Bedford, MA). A 10 μL aliquot of each filtered sample was injected onto a PRP-X300 anion exclusion column (250 mm × 4.1 mm, 7 μm particle size; Hamilton, Reno, NV) in 0.5 mN H_2SO_4/7% acetonitrile/93% water mobile phase. The column was developed (isocratically) at a flow rate of 0.5 mL/min. The eluate was passed through a Waters (Milford, MA) MicroMass ZQ 2000 mass spectrometer operating with electrospray ionization in the negative-ion mode. Single-ion monitoring at *m*/*z* 193 (M− for DG) was performed during elution, and the area under the peak (centered at 3.8 min) was determined. A standard curve of peak area versus DG concentration was generated by identical analysis of samples with known DG concentrations.

Quantitation of DG after Reaction of MIOX(II/II)·MI and MIOX(II/III)·MI with Limiting O_2. MIOX(II/II) was prepared by mixing iron-free MIOX, Fe(II), and Asc. This solution was divided into two equal aliquots. One aliquot was further divided into two samples, and [U-^{14}C]MI (∼70 nCi) was added to each to give final concentrations of 1−2 mM MIOX(II/II), 4 mM Asc, and 10 mM MI. To one of these samples (the control) was added an aliquot of O_2-free buffer with continuous gentle vortexing. To the other was added an aliquot of air-saturated (at either 5 or 23 °C) buffer with continuous gentle vortexing. After incubation at ambient

temperature (~23 °C) for a few minutes to allow the reactions to reach completion, the samples were incubated at 95 °C for several minutes to inactivate the enzyme. After centrifugation to pellet the denatured protein, the supernatant was subjected to the chromatographic procedure described in the next paragraph. The remainder of the original MIOX solution was subjected to the O_2-diffusion treatment to enrich in MIOX(II/III). This sample was divided into two aliquots, and after the cuvette was vented to the anoxic atmosphere to allow for dispersion of the remaining O_2(g), [U-^{14}C]MI (~70 nCi) was added to each to give final concentrations of 1−2 mM MIOX, 4 mM Asc, and 10 mM MI. The magnitudes of the changes in the absorption spectra of these samples during O_2 diffusion imply that they should have contained 0.5 ± 0.1 equiv of MIOX(II/III)·MI relative to total MIOX protein. To one of these samples (the control) was added an aliquot of O_2-free buffer with continuous gentle vortexing. To the other was added an equivalent aliquot of air-saturated (5 °C) buffer. The samples were incubated at ambient temperature for 5 min and then inactivated by incubation at 95 °C. The denatured protein was removed by centrifugation, and the supernatant was analyzed chromatographically.

The supernatant of each inactivated sample was loaded onto a 1 mL column of AG1-X8 resin (hydroxide form) packed in a 3 mL disposable syringe fritted with glass wool. The column was washed with 15 mL of H_2O while 1 mL fractions were collected. This wash eluted unreacted [U-^{14}C]-MI (corroborated by mass spectral analysis with unlabeled substrate). The column was then washed with 9 mL of 1 M HCl while 1 mL fractions were collected. This procedure eluted the [^{14}C]DG product (again, corroborated by mass spectrometry). Fractions were subjected to liquid scintillation counting to quantify the substrate and product. A control experiment, in which a similar assay mix was incubated under an air atmosphere for an extended time, showed that >96% of the substrate could be consumed. The total radioactivity in the product fractions from a given control sample, which was not significantly greater than the "background" radioactivity in the absence of enzyme, was subtracted from that for the corresponding experimental sample to quantify the product in the experimental sample.

RESULTS

Reaction of MIOX(II/II)·MI with Limiting O_2 Produces MIOX(II/III)·MI as a Stable Product. As all diiron oxygenases characterized to date activate O_2 from the II/II manifold (*6*−*10*), MIOX(II/II)·MI was initially considered the most likely candidate for the O_2-reactive enzyme form. Because the MIOX reaction is, unlike the previously characterized diiron−oxygenase reactions, charge-balanced without exogenous reducing equivalents (*2*), it was predicted that the reactive form should be regenerated following a single turnover with limiting O_2 in the presence of excess MI. To test this prediction for the case of the fully reduced enzyme, an O_2-free solution expected to contain MIOX(II/II)·MI [1.1 mM MIOX, 2 equiv of Fe(II), and 50 mM MI] was mixed with an equal volume of an air-saturated (at 5 °C) buffer solution (~0.3 mM O_2), and the state of the enzyme was assessed by EPR after completion of the reaction. The EPR spectrum of the control sample prepared by mixing the MIOX(II/II)·MI solution with O_2-free buffer (Figure 1A) is

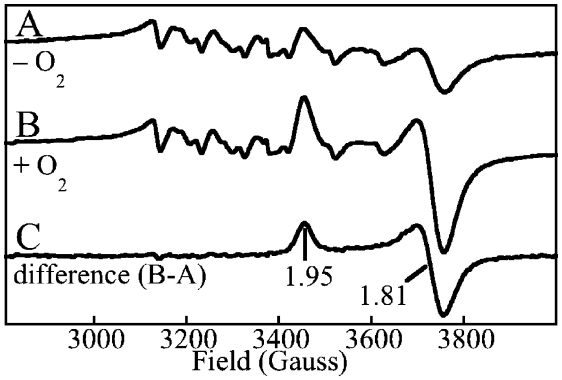

FIGURE 1: X-Band EPR spectra showing formation of MIOX(II/III)·MI as a stable product upon reaction of MIOX(II/II)·MI with limiting O_2. An O_2-free solution of MIOX, 2 equiv of Fe(II), and MI was mixed at 5 °C with an equal volume of (A) O_2-free buffer or (B) air-saturated (5 °C) buffer, and the reaction was allowed to proceed to completion before the sample was frozen in an EPR tube. The reactant concentrations after mixing were 0.53 mM MIOX, 1.06 mM Fe(II), 25 mM MI, and ~0 mM O_2 (A) or 0.15 mM O_2 (B). The spectra were acquired at 19 K with a microwave frequency of 9.45 GHz, a microwave power of 0.10 mW, a modulation amplitude of 5 G, a modulation frequency of 100 kHz, a time constant of 327 ms, and a scan time of 167 s. Spectrum C is the result of subtracting spectrum A from spectrum B.

dominated by the sextet signal from a substoichiometric quantity of Mn(II) that copurifies with the enzyme. This Mn(II) is most likely a contaminant.[2] The weak contribution of the axial g = (1.95, 1.81, 1.81) signal of MIOX(II/III)·MI to spectrum A establishes that, when O_2 is not purposefully added, only a small quantity of the mixed-valent complex develops [presumably due to scavenging of O_2(g) from the atmosphere]. By contrast, the EPR spectrum of the experimental sample (spectrum B) shows that a significant quantity of MIOX(II/III)·MI is generated as a stable product in the reaction of the reduced enzyme with limiting O_2. From the integrated intensity of the (B − A) difference spectrum (spectrum C), the concentration of MIOX(II/III)·MI produced in the reaction was determined to be 0.17 ± 0.02 mM, giving a MIOX(II/III)·MI:O_2 stoichiometry of 1.1 ± 0.2. The failure of the reduced enzyme to be regenerated and its stoichiometric conversion to the mixed-valent form by the cosubstrate, O_2, suggest that MIOX(II/II) is not the catalytically relevant form.

Inactivity of MIOX(III/III) and Its Conversion to MIOX-(II/III) by Activating Reductants. The preceding paper (*5*) shows that treatment of MIOX(II/II) with excess O_2 or H_2O_2 generates MIOX(III/III). The activity of MIOX(III/III) so produced and the possibility that it is a catalytically relevant enzyme form were assessed. When assayed at 5 °C in the absence of a reductant and in the presence of 25 mM MI and ~300 μM O_2, samples of the enzyme shown by either Mössbauer or EPR spectroscopy to contain predominantly

[2] Integration of the sextet EPR signal from the iron-free MIOX suggests that 0.2−0.5 equiv of Mn(II) is present in all preparations that were examined. Unlike the EPR spectrum of the diiron(II/III) cluster, the spectrum attributed to Mn(II) is unaffected by addition of MI or DG, and its intensity does not vary with reaction time in the FQ EPR experiments. The iron-free MIOX is inactive in the absence of Fe(II), even in the presence of additional Mn(II). Moreover, inclusion of Mn(II) in the assay at a concentration equal to that of Fe(II) (from ≤1 to >1000 equiv of each relative to MIOX) has no effect on activity.

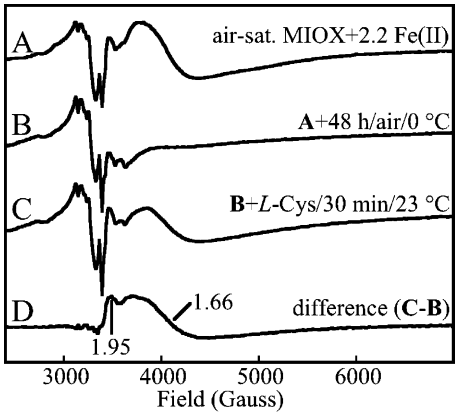

FIGURE 2: X-Band EPR spectra showing (A) production of ~0.3 equiv of MIOX(II/III) upon addition of 2.2 equiv of Fe(II) to air-saturated (0 °C) 1.2 mM iron-free MIOX, (B) decay of the mixed-valent state after a 48 h incubation at 0 °C in air, (C) regeneration of ~50% of the MIOX(II/III) upon treatment of the resulting MIOX(III/III) solution with 5 mM L-Cys for 30 min at 23 °C, and (D) the difference spectrum (C − B) associated with the L-Cys treatment. The spectra were recorded at 4 K (nominal temperature on an Oxford cryostat controller) with the following parameters: microwave frequency, 9.45 GHz; microwave power, 20 mW; modulation amplitude, 10 G; modulation frequency, 100 kHz; time constant, 327 ms; and scan time, 168 s.

(>95%) MIOX(III/III) exhibited very low activity (v/[MIOX] $\leq$ 0.01 s^{-1}), implying that MIOX(III/III) is not the active enzyme form.

It was previously reported that incubation of hog kidney MIOX (purified from its original source) with L-Cys and Fe(II) resulted in time-dependent activation (*11*). In addition, thiol compounds including L-Cys were reported to accelerate turnover in the steady state (*11*). To evaluate the possibility that these observations could have reflected reduction of inactive MIOX(III/III) emerging from the extensive purification procedure to the active form, the effects of both L-Cys and the additional, potentially physiologically relevant reductant, ascorbate, on the activity of MIOX(III/III) were assessed. Treatment of MIOX(III/III) with either 10 mM L-Cys or 10 mM Asc in the absence of O_2 for 1 h at 10 °C or 2 h at 5 °C was found to activate the enzyme by ~50-fold (v/[MIOX] = 0.4−0.5 s^{-1} under the same assay conditions, V_{max}/[MIOX] = 0.67 s^{-1}). Moreover, after this treatment, activity became almost independent of additional reductant in the assay (<10% enhancement in their presence) over at least 50 turnovers. By contrast, the activity of MIOX(III/III) that was not pretreated with either L-Cys or Asc was enhanced ~10-fold (v/[MIOX] ~ 0.1 s^{-1}) by the presence of 4 mM ascorbate and 1 mM Fe(II) over a similar assay time.[3]

The effect of the reductants on the oxidation state of the enzyme was then examined. In one experiment, addition of 2.2 equiv of Fe(II) to an air-saturated solution of 1.2 mM iron-free MIOX resulted in formation of a significant quantity (0.3 equiv) of MIOX(II/III), as revealed by its broad, axial **g** = (1.95, 1.66, 1.66) EPR signal at ~4 K and 20 mW (Figure 2A). Incubation of this sample at 0 °C in air for 48 h resulted in decay of the broad axial signal to undetectable levels (spectrum B). During this decay, no precipitation of protein or Fe(III) (i.e., rust) was observed, and the absorption spectrum of the sample evolved to that characteristic of MIOX(III/III) (not shown). The long time required for complete decay indicates that, once formed, MIOX(II/III) is reasonably stable in the presence of O_2. Treatment of the resulting MIOX(III/III) with 5 mM L-Cys at 23 °C for 30 min regenerated approximately half of the original yield of MIOX(II/III) (spectra C and D). In other experiments, treatment of MIOX(III/III) with 10 mM L-Cys at 10 °C for 2 h resulted in production of 0.6 ± 0.2 equiv of MIOX(II/III), and reduction of MIOX(III/III) by Asc was also demonstrated (not shown). Thus, L-Cys and Asc convert MIOX(III/III) to MIOX(II/III) and activate the enzyme.

Preparation of MIOX(II/III) and Binding of MI Monitored by Absorption Spectroscopy. The conversion by reaction components (O_2 and activating reductant) of both MIOX(II/II) and MIOX(III/III) to MIOX(II/III) (Figures 1 and 2) suggests that the mixed-valent complex could be the catalytically relevant enzyme form. To test this notion, a method for preparing the mixed-valent complex was required. As suggested by the results of Figures 1 and 2, treatment of the reduced enzyme simultaneously with O_2 and activating reductant (L-Cys or ascorbate) leads to convergence on the mixed-valent state, allowing it to be prepared in high yield. Slow diffusion of O_2(g) into a solution of MIOX, 2 equiv of Fe(II), and 5 mM Asc (or L-Cys; not shown) results in the gradual development of UV−visible absorption features at ~340 and ~500 nm (Figure 3A, dotted spectra). With prolonged incubation and repeated gentle mixing, the spectrum eventually becomes stable, indicating that completion or steady state is achieved. Subsequent addition of MI [after dispersion of unreacted O_2(g)] generates MIOX(II/III)·MI with a yield of up to 0.6 equiv (as shown by both Mössbauer and EPR quantitation) and results in a decrease in the absorption in the ~340 and ~500 nm region of the spectrum and an increase in absorption in the ~400 nm region (Figure 3A, solid spectrum). The difference spectrum for substrate addition (Figure 3A, inset) has a distinct minimum at ~495 nm, corresponding to absorption from MIOX(II/III) that is lost upon binding of MI, and a maximum at ~390 nm, corresponding to absorption from MIOX(II/III)·MI that develops. The kinetics of binding of MI to MIOX(II/III) reflected by the loss of absorbance at 495 nm (ΔA_{495}) are complex (Figure 3B). It is not yet clear whether this kinetic complexity reflects multistep binding to MIOX(II/III), binding of MI to multiple forms of the enzyme, or a combination of both. For example, MI binds to MIOX(III/III) comparatively slowly (Figure S2B of the Supporting Information) and weakly (requiring many tens of millimolar to reach saturation), causing a decrease in A_{495} (Figure S2A of the Supporting Information) of a magnitude similar to that caused by binding to the mixed-valent form. Thus, the very slow (k ~ 0.04 s^{-1}) phase of relatively small amplitude that is most prevalent in the high-MI traces of Figure 3B could reflect binding to MIOX(III/III) generated as a "contaminant" in preparation of the desired mixed-valent form. The data were analyzed as the sum of exponential decay terms. The traces from the reactions with lower MI concentrations [1 (○), 3 (□), and 10 mM (◇)] are satisfactorily analyzed as two parallel decay processes, whereas the traces from reactions with higher MI concentrations [30 (△) and 100 mM (+)]

[3] Presumably, the enzyme velocity should increase with reaction time under these conditions, but this expectation has not yet been accurately evaluated.

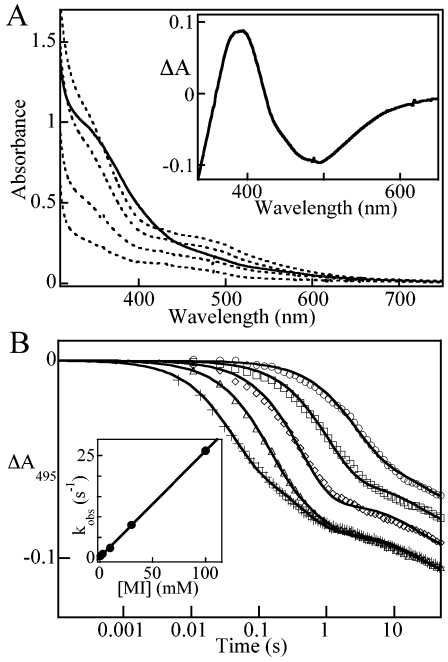

FIGURE 3: Preparation of MIOX(II/III) and MIOX(II/III)·MI monitored by optical absorption spectroscopy. (A) Absorption spectra during slow diffusion (at 10 °C) of O_2(g) into a solution of 0.50 mM MIOX, Fe(II) (1.8 equiv) and ascorbate (4 mM) (···) and after subsequent dispersion of unreacted O_2(g) and addition of MI to 9 mM (—). The inset in panel A shows the change in the spectrum associated with addition of MI. (B) Kinetics of absorbance at 495 nm after mixing (at 5 °C) of a solution enriched in MIOX(II/III) (as in panel A but with 0.92 mM MIOX) with an equal volume of an O_2-free solution of MI to give a final MI concentration of 1 (○), 3 (□), 10 (◇), 30 (△), or 100 mM (+). The solid lines are fits of the equation for either two (○, □, and ◇) or three (△ and +) parallel, first-order decay processes to the data. The inset in panel B is a plot of the rate constant for the fastest phase obtained in each fit versus [MI] (●) with a linear fit (—), which has a slope of 2.6×10^2 M^{-1} s^{-1} and an intercept of 0.1 s^{-1}.

require three exponential terms. A plot of the apparent first-order rate constant for the fastest phase (which has the largest amplitude) versus MI concentration yields a line with a slope of 2.6×10^2 M^{-1} s^{-1} and an intercept of ~0.1 s^{-1} (Figure 3B, inset), from which a dissociation constant (K_D) of ~0.4 mM would be estimated. We emphasize that the simple mechanism for substrate binding implied by this analysis (one-step, reversible addition with the rate and equilibrium constants given) does not adequately account for the data: further characterization of the binding reaction is required. Nevertheless, the analysis indicates that the binding of MI to MIOX(II/III) reflected by the change in the absorption spectrum is sufficiently fast to be part of the catalytic cycle (V_{max}/[MIOX] = 0.67 ± 0.06 s^{-1}, $K_{M,apparent}$ = 12 ± 4 mM at 5 °C and ~0.3 mM O_2). For example, at 10 mM MI, binding should occur with an effective first-order rate constant of 2.6 s^{-1}, faster than the observed v/[MIOX] of 0.3 s^{-1}.

Cyclic Reaction of MIOX(II/III)·MI with Limiting O_2. The functional significance of the MIOX(II/III)·MI complex thus prepared was assessed by SF absorption and FQ EPR experiments in which it was mixed with limiting O_2. Time-dependent absorption difference spectra acquired after the mix (Figure 4A) show transient features at the same wavelengths as, but opposite in sign to, the features in the difference spectrum associated with binding of MI to

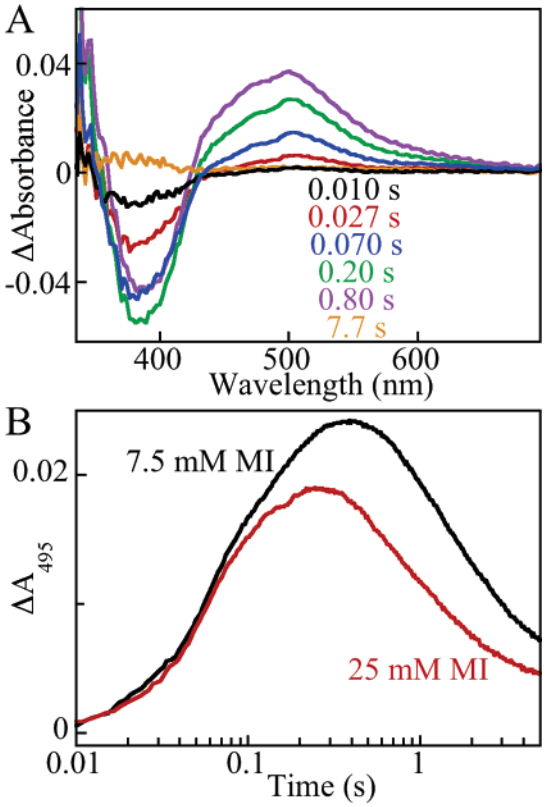

FIGURE 4: Reaction of MIOX(II/III)·MI with limiting O_2 monitored by SF absorption spectroscopy. MIOX(II/III)·MI was prepared as described in Materials and Methods. This solution was mixed in a 1:1 volume ratio with air-saturated (at 5 °C in panel A and 23 °C in panel B) buffer. (A) The concentrations after mixing were 0.50 mM total MIOX, ~0.3 mM MIOX(II/III)·MI (estimated as described in Materials and Methods), 0.15 mM O_2, and 7.2 mM free MI. The spectra reflect the changes occurring between the reaction time of the first reliable spectrum (0.003 s) and reaction times of 0.010 (black), 0.027 (red), 0.070 (blue), 0.20 (green), 0.80 (purple), and 7.7 s (orange). (B) The concentrations after mixing were 0.50 mM total MIOX, ~0.3 mM MIOX(II/III)·MI, 0.10 mM O_2, and either 7.2 mM (black trace) or 25 mM (red trace) free MI.

MIOX(II/III) (Figure 3A, inset). A negative feature at ~390 nm develops rapidly (black and red spectra), implying that the MIOX(II/III)·MI complex is consumed, and a positive difference feature at ~495 nm develops soon after (red, blue, green, and purple spectra), suggesting that MI-free MIOX(II/III) is then produced. Upon completion of the reaction, difference absorption decays almost completely (Figure 4, orange spectrum), suggesting that the starting MIOX(II/III)·MI complex is regenerated. Decay of the positive feature at 495 nm is faster, and the maximum absorbance is consequently diminished at higher MI concentrations (Figure 4B). Because an increase in the concentration of free MI should specifically accelerate binding of the substrate, this observation establishes that MIOX(II/III) does indeed accumulate during the reaction, consistent with the hypothesis that turnover occurs. The temporal separation between development of the negative 390 nm and positive 495 nm features implies that at least one intermediate state accumulates between MIOX(II/III)·MI and MIOX(II/III).

EPR spectra of samples frozen before, during, and after the reaction confirm that MIOX(II/III)·MI reacts rapidly with O_2 and is subsequently regenerated (Figure 5). The intensities of the axial **g** = (1.95, 1.81, 1.81) signal from (non-freeze-

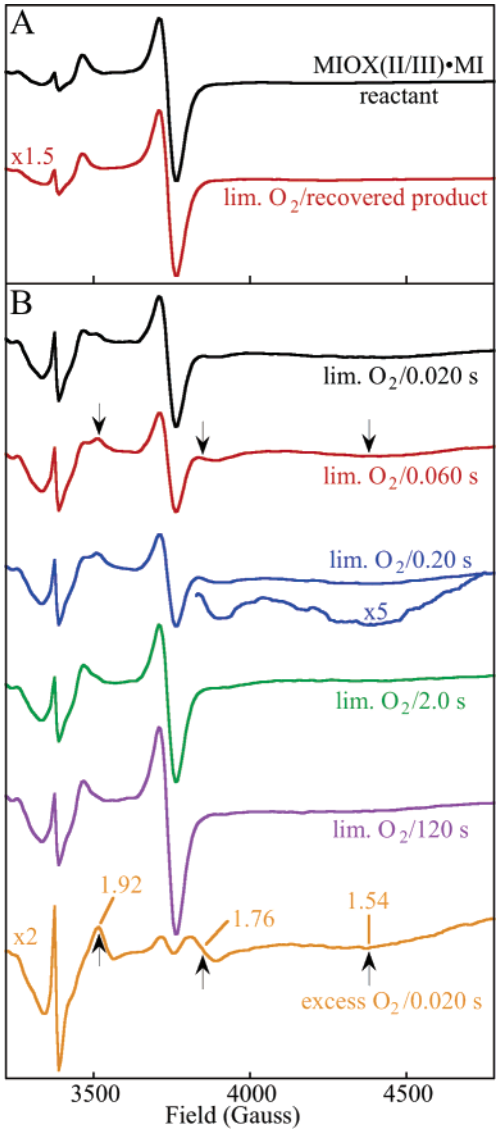

FIGURE 5: Reaction of MIOX(II/III)·MI with O_2 monitored by FQ EPR spectroscopy. The preparation of the 0.56 mM MIOX(II/III)·MI solution is described in Materials and Methods. This solution was mixed either with 0.5 equiv volumes of 0.58 mM O_2 (lim. O_2) or with 2 equiv volumes of 1.4 mM O_2 (excess O_2), as described in Materials and Methods. (A) Spectra of the MIOX(II/III)·MI reactant solution (black spectrum) and the recovered product of the lim. O_2 reaction (red spectrum). (B) Spectra of samples freeze-quenched at various reaction times during the lim. O_2 reaction (black, red, blue, green, and purple spectra) and at 0.020 s of the excess O_2 reaction (orange spectrum). The spectra were acquired at 4 K (nominal temperature on an Oxford cryostat controller) with a microwave frequency of 9.45 GHz, a microwave power of 20 mW, a modulation frequency of 100 kHz, a modulation amplitude of 10 G, a time constant of 327 ms, and a scan time of 167 s. The sharp feature at 3380 G ($g = 2.00$) seen in all spectra is intrinsic to the EPR cavity.

quenched) samples of the reactant (Figure 5A, black spectrum) and recovered product (red spectrum) are identical, after scaling to account for the 33% reduction in the MIOX concentration of the latter resulting from the 2:1 mix with the O_2-containing buffer. Spectra of samples freeze-quenched during the reaction (Figure 5B) show that the signal decays and redevelops (compare black, red, blue, green, and purple spectra) with kinetics [Figure 6(○)] very similar to those reflected by the absorbance at 390 nm in the most comparable SF experiments [Figure 6 (···)]. In reaction of the complex

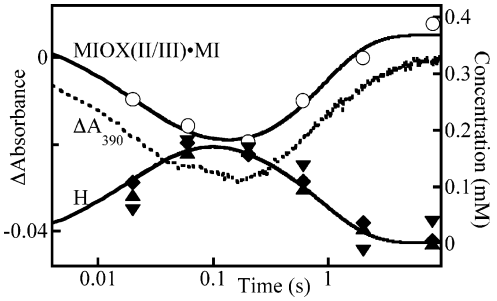

FIGURE 6: Kinetics of absorbance at 390 nm (···, left *y*-axis) in the 25 mM MI experiment of Figure 4B and of [MIOX(II/III)·MI] (○, right *y*-axis) and [**H**] (▲, ▼, and ◆, right *y*-axis) in the lim. O_2 reaction of Figure 5. Calculation of concentrations from the intensities of the EPR features is described in Materials and Methods and Supporting Information. The upward triangles, diamonds, and downward triangles represent the intensities of the $g = 1.92$, 1.76, and 1.54 features, respectively. The solid lines are simulations of the kinetic data according to Scheme 1.

with excess O_2 (0.95 mM), the axial signal decays by ~80% in just 0.020 s (Figure 5B, orange spectrum), and three new features (upward-pointing arrows) develop at 3510, 3840, and ~4380 G ($g = 1.92$, 1.76, and ~1.54, respectively). In the spectra from the limiting-O_2 reaction, these same features (downward-pointing arrows and "blow-up" of the blue spectrum in Figure 5B) can be seen to develop and decay together (compare triangles and diamonds in Figure 6). They represent the components of a broad, rhombic signal of an accumulating intermediate, as anticipated from the SF data. This intermediate, which we denote **H**, is unlikely to be merely the MIOX(II/III)·DG complex, as addition of 100 mM DG to a sample enriched in MIOX(II/III) was found to elicit a distinct, much broader rhombic signal [**g** ~ (1.95, 1.72, 1.16); Figure S3 of the Supporting Information].[4] The intensities of the three features of the rhombic signal of **H** (see Figure S4 of the Supporting Information for explanation of the "peak-height" treatment used to measure them) define its kinetics in relative terms, and the assumption that it forms from MIOX(II/III)·MI and O_2 allows the relative EPR intensities to be related to absolute concentrations (see Materials and Methods for how this is done). The kinetics of the MIOX(II/III)·MI reactant [Figure 6 (○)] and **H** (▲, ▼, and ◆) so defined can be simulated (solid lines) by using the mechanism and rate constants shown in Scheme 1. In this mechanism, it is assumed that **H** is not the product complex, as suggested by the failure of addition of DG to MIOX(II/III) to elicit the EPR signature of **H**. A MIOX(II/III)·DG complex is presumed to occur between **H** and MIOX(II/III), but the minimal temporal separation between the decay of the signal of **H** and redevelopment of the axial signal of MIOX(II/III)·MI implies that the product complex must dissociate more rapidly than it forms from **H** (a rate constant of 8 s^{-1} has been assumed for simulations, but the data do not allow an upper bound to be set for this value) and, therefore, accumulate minimally if at all. Scheme 1 predicts that $V_{max}/[MIOX] = 1.0 \pm 0.2$ s^{-1} under the

[4] This observation strongly suggests but is not rigorous proof that **H** is not the product complex. DG is produced by MIOX in acyclic form (*16*) but exists in solution predominantly in cyclic (hemiacetal) form (*17*). It is conceivable that the cyclic form could bind with comparable affinity but elicit an EPR signal different from that of the complex with the acyclic form.

Scheme 1: Kinetic Mechanism Used in the Simulations of Figure 6 (solid lines)[a]

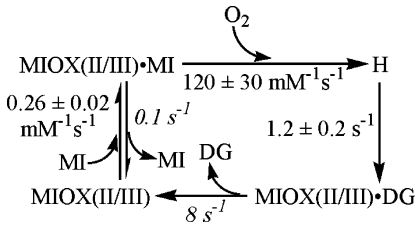

[a] Rate constants that have not yet been determined well are shown in italics. The error limits for the other rate constants are estimates based on iterative simulation of all the data and visual evaluation of agreement.

conditions of the assay, but correction to the maximal observed fraction of the active, mixed-valent state (0.6) yields a predicted V_{max}/[MIOX] of 0.6 ± 0.1 s^{-1}, in agreement with the measured value. In other words, the observed spectral changes are sufficiently rapid to be associated with steps on the catalytic pathway, consistent with the hypothesis that MIOX(II/III)•MI activates O_2 for DG production.

Radiometric Assay for DG Production in Reactions of MIOX(II/II)•MI and MIOX(II/III)•MI with Limiting O_2. The production of DG in the reaction of MIOX(II/III)•MI with limiting O_2 was verified, and the possibility that reaction of MIOX(II/II)•MI might also be productive was assessed by end-point assays employing [U-^{14}C]MI. In three replicate experiments in which a solution containing 1.0 mM total MIOX and ~0.5 mM MIOX(II/III)•MI was manually mixed with slightly more than an equal volume of air-saturated (5 °C) buffer (giving 0.48 mM MIOX and 0.16 ± 0.01 mM O_2), 0.123 ± 0.005 mM (mean ± range) DG was detected. This corresponds to a DG:O_2 stoichiometry of 0.8 ± 0.1, similar to the theoretical and experimentally verified (*2*) value of 1. The small deviation from the theoretical value could reflect incomplete recovery in the chromatographic procedure or uncoupled O_2 reduction in a fraction of events under these single-turnover conditions (e.g., by its reaction with a fraction of enzyme still in the II/II oxidation state; vide infra). By comparison, only 0.076 ± 0.005 mM was detected when the reduced MIOX was not first converted to the mixed-valent form before being mixed with the O_2-containing buffer. Thus, only 0.62 as much product (0.5 DG/O_2) was generated by the reduced enzyme reactant than by the enzyme that had been pretreated to accumulate the mixed-valent form. The greater yield of product from the mixed-valent enzyme was not a result of O_2 remaining from the O_2-diffusion treatment. This treatment was carried out prior to addition of the labeled MI, and control samples (prepared by mixing the MIOX•[U-^{14}C]MI reactant with O_2-free buffer) for both reduced and mixed-valent reactant forms were also analyzed and found to contain only background levels of radioactivity in the DG fractions.

The formation of DG from the reduced enzyme could indicate that its reaction with O_2 is also productive in some fraction of events. Alternatively, initial conversion by O_2 of a fraction of the MIOX(II/II)•MI to MIOX(II/III)•MI (as demonstrated in Figure 1) and subsequent turnover by the mixed-valent form might be responsible for the product in this reaction. In an attempt to distinguish these scenarios, the O_2:MIOX ratio was varied in two additional experiments. When the O_2:MIOX ratio was increased from 0.33 to 0.46 by a decrease in the MIOX concentration to 0.3 mM, the ratio of DG from the reduced and mixed-valent reactants increased to 0.78, while the DG:O_2 stoichiometry for the MIOX(II/III)•MI reaction remained unchanged (0.8). When the reactant ratio was decreased to 0.05 by an increase in the MIOX concentration to 1.3 mM and a decrease in the O_2 concentration to 0.068 mM, the product ratio decreased to 0.56 and the DG:O_2 stoichiometry for the MIOX(II/III)•MI reaction was again 0.8. The data suggest that, as carried out in these experiments, the ratio of product from the reduced and mixed-valent enzyme forms approaches 0.5 as [O_2]/[MIOX] approaches zero. The fact that these experiments were carried out by manual mixing of the O_2 and MIOX•MI reactant solutions warrants emphasis. Given that sequential conversion of MIOX(II/II)•MI to MIOX(II/III)•MI and turnover by the mixed-valent complex is a possibility, accurate assessment of product yield from the reduced enzyme may (depending on the kinetics of the various steps) require rapid mixing to ensure that homogeneity of the reaction solution is achieved before any reaction occurs.

DISCUSSION

Evidence that MIOX(II/II) Is Not the Catalytically Active Enzyme Form. In one possible mechanism for the MIOX reaction [suggested by extensive precedent from other non-heme diiron oxygenases and oxidases (*6*−*10*)], O_2 could react with MIOX(II/II)•MI to generate a high-valent intermediate that could initiate MI oxidation by abstraction of hydrogen, presumably from C1 (as this is the only C−H bond that is obviously cleaved in the reaction). The reaction stoichiometry (*2*) would require that subsequent steps regenerate MIOX(II/II). The failure of the reduced enzyme to be regenerated following its reaction with limiting O_2 implies that it cannot be the *catalytic* enzyme form.

Evidence that MIOX(III/III) Is Not the Catalytically Active Form. In a second possible mechanism [favored by Hamilton and co-workers (*18*)], MI would reduce the enzyme by two electrons, in the process generating a 1-keto form of the substrate (*myo*-inosose-1). The obvious place for the electrons to reside in the reduced enzyme would be the diiron cluster. Thus, MIOX(III/III)•MI could convert to MIOX(II/II)•*myo*-inosose-1. Reduction of O_2 by the diiron(II/II) cluster to a nucleophilic peroxide that would attack the carbonyl of the ketone intermediate would generate a 1-(hydro)peroxy-MI intermediate. Chemical precedent suggests that this intermediate could decompose to DG (*11*, *19*−*21*), leading to incorporation of a single O atom from O_2 into the C1-derived carboxylate, as has been shown to occur in the MIOX reaction (*3*, *22*). We rule out this pathway for the MIOX reaction on the basis of the following considerations. First, spectra in the preceding paer (*5*) demonstrate that addition of MI to MIOX(III/III) perturbs its Mössbauer spectrum but does not change its oxidation state (*5*). Second, the binding of MI to MIOX(III/III) is too slow (Figure S2 of the Supporting Information) and weak to account for the rate and MI concentration dependence of the catalytic reaction. Third, it has been reported that H_2O_2, which converts MIOX(II/II) to MIOX(III/III), inactivates the enzyme (*11*) and that catalase therefore protects it (*18*). Fourth (and most importantly), MIOX(III/III) has very low activity (<2% of maximum) but can be fully reactivated by treatment with reductants such as L-Cys that convert it to MIOX(II/III).

Evidence that MIOX(II/III) Is the Catalytically Active Form. The propensity of MIOX(II/III) to accumulate in the presence of O_2 and L-Cys, the former a substrate and the latter reported by Hamilton and co-workers to activate MIOX (*11*), hinted that the mixed-valent state might be the catalytic enzyme form. The demonstrations of (1) cyclic decay and regeneration of MIOX(II/III)·MI upon its mixing with limiting O_2 and (2) DG production with an O_2 stoichiometry similar to the theoretical and experimentally confirmed (*2*) value of 1 prove that the mixed-valent form is indeed catalytically competent. The complete incompetence of the fully reduced form is less certain, as the smaller quantity of product observed after its single-turnover reaction could have arisen either directly from reaction of O_2 with MIOX(II/II)·MI in a fraction of events or indirectly by sequential conversion to the mixed-valent complex and turnover by this form. Clarification of this point will require experiments that define the kinetics of conversion of MIOX(II/II)·MI to MIOX(II/III)·MI and of product formation in the reactions of both reduced and mixed-valent enzyme forms.

Implications of the Use of the Mixed-Valent Diiron Cluster. If the reduced enzyme should prove to be incompetent for DG production, it would imply that its reaction with O_2 to generate the mixed-valent state is an *activation* step. The details of this process, including whether the mixed-valent form is produced directly or by comproportionation of the reactant MIOX(II/II) with a MIOX(III/III) intermediate and the identity of the O_2-derived product, warrant further investigation.

The use of the diiron(II/III) cofactor can rationalize several of the previously reported complex kinetic characteristics of MIOX. Most notably, the activation [both time-dependent activation and enhancement of activity in the steady state (*11*)] by thiols such as L-Cys, despite the absence of a stoichiometric requirement for electrons (*2*), can be explained by their conversion of inactive MIOX(III/III) to active MIOX(II/III). Indeed, spectrophotometric monitoring of the conversion of the fully oxidized enzyme to the mixed-valent state by 5 mM L-Cys showed that the process is slow, requiring tens of minutes at 23 °C to approach completion. This time scale seems consistent with the 5−10 min at 30 °C required for the time-dependent activation of the hog kidney enzyme (purified from its natural source) by L-Cys (*11*).

The use of the mixed-valent state also creates the possibility for redox regulation of MIOX activity in physiological contexts. The established links between diabetic pathologies and oxidative stress (*23*) and the circumstantial links of derangements in MI metabolism to these pathologies (*24* and references cited therein) make this possibility provocative.

Possible Mechanisms for O_2 Activation and DG Production by MIOX(II/III)·MI. By what mechanism might the diiron(II/III) cofactor activate O_2 for the unique glycol-cleavage reaction? Addition of O_2 to the diiron(II/III) cluster to form a peroxide and subsequent O−O cleavage (a la the canonical diiron oxygenase mechanism) would, without injection of one or more electron by an exogenous reductant [which would seem to be ruled out by the reaction stoichiometry (*2*)], generate an unprecedented diiron(IV/V) complex. This possibility seems remote. One possible mechanism that would obviate this unappealing step would involve C1−H cleavage by the initial diiron(II/III)−O_2 adduct, formally a (superoxo)diiron(III/III) complex (Scheme 2). If

Scheme 2: Possible Mechanism for Conversion of MI to DG Initiated by Addition of O_2 to MIOX(II/III)·MI and Cleavage of the C1−H Bond by the Resulting Formally (Superoxo)diiron(III/III) Complex

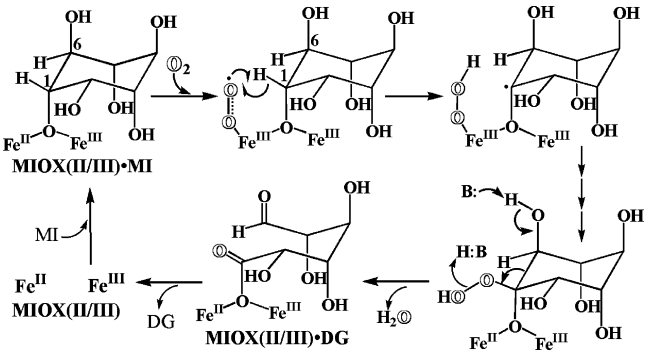

C1−H bond cleavage were to occur homolytically (i.e., by H-atom abstraction), a (hydroperoxo)diiron(III/III) complex would be generated. Transfer of the hydroperoxide unit, intact, from the diiron intermediate to the substrate C1 radical (in a single step or by one of several possible multistep mechanisms) would generate the 1-hydroperoxy-MI intermediate envisioned by Hamilton and co-workers (*18*). Alternative mechanisms (for example, involving formal hydroxylation of C1) can also be envisioned.

Is cleavage of the C1−H bond by the hypothetical metal-superoxide intermediate thermodynamically feasible? There is no direct chemical precedent to establish that it is, but recent studies suggest that it might be. (Superoxo)copper(II) complexes have recently been invoked as the hydrogen-atom-abstracting intermediates in the reactions of dopamine β-monooxygenase (DβM) (*25*) and peptidyl glycine α-amidating monooxygenase (PAM) (*26*), which use two well-separated and uncoupled copper(I) ions for O_2 activation and aliphatic hydroxylations. For PAM, the evidence is primarily computational (*26*), although a recent X-ray crystallographic study of the reduced enzyme in complex with a poor substrate attributed electron density near the Cu_M center to bound O_2 (*27*), implying that the complex characterized might represent the H• abstracting (superoxo)copper(II) intermediate. For DβM, slowing of Cu(I) oxidation with a fluorine-substituted substrate was interpreted in terms of kinetic coupling of O_2 activation and C−H cleavage, which was rationalized by reversible formation of a disfavored (superoxo)copper(II) complex that effects H• abstraction (*25*). More recently, Que and co-workers presented evidence that the (superoxo)diiron(II/III) complex formed by addition of O_2 to an inorganic diiron(II/II) complex [most likely in "end-on" fashion to a single Fe(II)] can undergo coupled proton and electron transfer from 2,4-di-*tert*-butylphenol (*28*). Because it is one electron more oxidized than the Que superoxide complex, the postulated (superoxo)diiron(III/III) complex in MIOX might be even more potent as a (formal) H• acceptor as a result of a greater reduction potential. Conversely, the model study underscores the possibility that fully reduced MIOX could theoretically activate O_2 for DG production by the same mechanism postulated for the mixed-valent form, emphasizing the need for the aforementioned kinetic experiments to address the competence of the reduced form more definitively.

Chemical Logic of the Use of the Mixed-Valent Diiron Cluster for O_2 Activation. The proposed novel mechanisms

for O_2 activation and C1−H bond cleavage would rationalize the use of the diiron(II/III) cluster [as opposed to a mononuclear iron(II) or diiron(II/II) center] as the catalytic cofactor. The mixed-valent form could be incapable of promoting cleavage of the O−O bond, thereby allowing all four oxidizing equivalents of O_2 to be transferred to the substrate in what would formally be a hydroperoxyl-radical-rebound step. In addition, whereas a sequence of Fe(III)-superoxide formation, H• abstraction, and hydroperoxyl-radical rebound would not, a priori, require a diiron center, the second iron [the Fe(III) site] could be required for Lewis acidity to promote ionization of the C1 hydroxyl group. Formation of the C1 alkoxide could activate for C1−H cleavage and might be necessary to allow the superoxide complex to effect this step.

Conclusions. The cyclic and productive reaction of MIOX-(II/III)·MI with O_2, with kinetics fast enough to account for the catalytic rate, establishes that MIOX can use a diiron-(II/III) cluster as its catalytic cofactor, implying that it is a novel member of the non-heme diiron oxygenase family. The sequence of events leading from the diiron(II/III)-O_2 adduct to DG production remains to be established. Elucidation of the nature of intermediate **H** will provide important clues in this regard. The fact that decay of **H** appears to be the slowest step in the catalytic cycle, permitting its accumulation to a concentration approaching that of the starting MIOX(II/III)·MI complex, and its resolved EPR features bode well for its characterization by electron−nuclear double-resonance methods. In addition, examination of the effect of deuterium substitution on the kinetics of formation and decay of the intermediate may inform with regard to its position in the catalytic cycle (*29*).

ACKNOWLEDGMENT

We thank Dr. Gordon A. Hamilton, whose spirit of discovery and fascination with oxygenases infused this work.

SUPPORTING INFORMATION AVAILABLE

Determination of O_2 concentrations in reactant solutions (procedure and Figure S1); absorption spectrum of MIOX-(III/III), changes caused by binding of MI, and kinetics of the binding reaction (Figure S2); comparison of the EPR spectra of a sample prepared by addition of 100 mM DG to MIOX(II/III) to that of a sample containing intermediate **H** (Figure S3); and determination of the intensities of the EPR features of **H** in the spectra of freeze-quenched samples (procedure and Figure S4). This material is available free of charge via the Internet at http://pubs.acs.org.

REFERENCES

1. Charalampous, F. C., and Lyras, C. (1957) Biochemical studies on inositol. IV. Conversion of inositol to glucuronic acid by rat kidney extracts, *J. Biol. Chem. 228*, 1−13.
2. Charalampous, F. C. (1959) Biochemical studies on inositol. V. Purification and properties of the enzyme that cleaves inositol to D-glucuronic acid, *J. Biol. Chem. 234*, 220−227.
3. Moskala, R., Reddy, C. C., Minard, R. D., and Hamilton, G. A. (1981) An oxygen-18 tracer investigation of the mechanism of *myo*-inositol oxygenase, *Biochem. Biophys. Res. Commun. 99*, 107−113.
4. Hankes, L. V., Politzer, W. M., Touster, O., and Anderson, L. (1969) *myo*-Inositol catabolism in human pentosurics: The predominant role of the glucuronate-xylulose-pentose phosphate pathway, *Ann. N.Y. Acad. Sci. 165*, 564−576.
5. Xing, G., Hoffart, L. M., Diao, Y., Prabhu, S. K., Arner, R. J., Reddy, C. C., Krebs, C., and Bollinger, J. M., Jr. (2006) A Coupled Dinuclear Iron Cluster that is Perturbed by Substrate Binding in *myo*-Inositol Oxygenase, *Biochemistry 45*, 5393−5401.
6. Wallar, B. J., and Lipscomb, J. D. (1996) Dioxygen activation by enzymes containing binuclear non-heme iron clusters, *Chem. Rev. 96*, 2625−2657.
7. Solomon, E. I., Brunold, T. C., Davis, M. I., Kemsley, J. N., Lee, S. K., Lehnert, N., Neese, F., Skulan, A. J., Yang, Y.-S., and Zhou, J. (2000) Geometric and Electronic Structure/Function Correlations in Non-Heme Iron Enzymes, *Chem. Rev. 100*, 235−349.
8. Merkx, M., Kopp, D. A., Sazinsky, M. H., Blazyk, J. L., Müller, J., and Lippard, S. J. (2001) Dioxygen activation and methane hydroxylation by soluble methane monooxygenase: A tale of two irons and three proteins, *Angew. Chem., Int. Ed. 40*, 2782−2807.
9. Fox, B. G., Lyle, K. S., and Rogge, C. E. (2004) Reactions of the Diiron Enzyme Stearoyl-Acyl Carrier Protein Desaturase, *Acc. Chem. Res. 37*, 421−429.
10. Krebs, C., Price, J. C., Baldwin, J., Saleh, L., Green, M. T., and Bollinger, J. M., Jr. (2005) Rapid Freeze-Quench ^{57}Fe Mössbauer Spectroscopy: Monitoring Changes of an Iron-Containing Active Site during a Biochemical Reaction, *Inorg. Chem. 44*, 742−757.
11. Reddy, C. C., Pierzchala, P. A., and Hamilton, G. A. (1981) *myo*-Inositol oxygenase from hog kidney. II. Catalytic properties of the homogeneous enzyme, *J. Biol. Chem. 256*, 8519−8524.
12. Price, J. C., Barr, E. W., Tirupati, B., Bollinger, J. M., Jr., and Krebs, C. (2003) The first direct characterization of a high-valent iron intermediate in the reaction of an α-ketoglutarate-dependent dioxygenase: A high-spin Fe(IV) complex in taurine/α-ketoglutarate dioxygenase (TauD) from *Escherichia coli*, *Biochemistry 42*, 7497−7508.
13. Aasa, R., and Vänngård, T. (1975) EPR signal intensity and powder shapes. Reexamination, *J. Magn. Reson. 19*, 308−315.
14. Bollinger, J. M., Jr., Tong, W. H., Ravi, N., Huynh, B. H., Edmondson, D. E., and Stubbe, J. (1994) Mechanism of assembly of the tyrosyl radical-diiron(III) cofactor of *E. coli* ribonucleotide reductase. 2. Kinetics of the excess Fe^{2+} reaction by optical, EPR, and Mössbauer spectroscopies, *J. Am. Chem. Soc. 116*, 8015−8023.
15. Bollinger, J. M., Jr., Tong, W. H., Ravi, N., Huynh, B. H., Edmondson, D. E., and Stubbe, J. (1995) Use of rapid kinetics methods to study the assembly of the diferric-tyrosyl radical cofactor of *E. coli* ribonucleotide reductase, *Methods Enzymol. 258*, 278−303.
16. Naber, N. I., and Hamilton, G. A. (1987) Concerning the mechanism for transfer of D-glucuronate from *myo*-inositol oxygenase to D-glucuronate reductase, *Biochim. Biophys. Acta 911*, 365−368.
17. Ramos, M. L. D., Caldeira, M. M. M., and Gil, V. M. S. (1996) NMR study of uronic acids and their complexation with molybdenum(VI) and tungsten(VI) oxoions, *Carbohydr. Res. 286*, 1−15.
18. Naber, N. I., Swan, J. S., and Hamilton, G. A. (1986) L-*myo*-Inosose-1 as a probable intermediate in the reaction catalyzed by *myo*-inositol oxygenase, *Biochemistry 25*, 7201−7207.
19. Hamilton, G. A. (1974) in *Chemical models and mechanisms for oxygenases* (Hayaishi, O., Ed.) pp 405−451, Academic Press Inc., New York.
20. Hamilton, G. A., Reddy, C. C., Swan, J. S., Moskala, R., Mulliez, E., Naber, N. I., Nozaki, M., Yamamoto, S., and Ishimura, Y. (1982) *Mechanistic aspects of oxygenases in general and myo-inositol oxygenase in particular*, pp 111−123, Academic Press Inc., New York.
21. Fraser, M. S., and Hamilton, G. A. (1982) Models for oxygenases that catalyze the cleavage of carbon−carbon bonds: Kinetics and mechanism of the decomposition of 2,3-dimethyl-3-peroxyindolenines in aqueous solution, *J. Am. Chem. Soc. 104*, 4203−4211.
22. Charalampous, F. C. (1960) Biochemical studies on inositol. VI. Mechanism of cleavage of inositol to D-glucuronic acid, *J. Biol. Chem. 235*, 1286−1291.
23. Evans, J. L., Goldfine, I. D., Maddux, B. A., and Grodsky, G. M. (2002) Oxidative stress and stress-activated signaling pathways: A unifying hypothesis of type 2 diabetes, *Endocr. Rev. 23*, 599−622.
24. Prabhu, K. S., Arner, R. J., Vunta, H., and Reddy, C. C. (2005) Up-regulation of human *myo*-inositol oxygenase by hyperosmotic stress in renal proximal tubular epithelial cells, *J. Biol. Chem. 280*, 19895−19901.

25. Evans, J. P., Ahn, K., and Klinman, J. P. (2003) Evidence that dioxygen and substrate activation are tightly coupled in dopamine β-monooxygenase: Implications for the reactive oxygen species, *J. Biol. Chem. 278*, 49691−49698.
26. Chen, P., and Solomon, E. I. (2004) Oxygen Activation by the Noncoupled Binuclear Copper Site in Peptidylglycine α-Hydroxylating Monooxygenase. Reaction Mechanism and Role of the Noncoupled Nature of the Active Site, *J. Am. Chem. Soc. 126*, 4991−5000.
27. Prigge, S. T., Eipper, B. A., Mains, R. E., and Amzel, L. M. (2004) Dioxygen binds end-on to mononuclear copper in a precatalytic enzyme complex, *Science 304*, 864−867.
28. Shan, X., and Que, L., Jr. (2005) Intermediates in the oxygenation of a nonheme diiron(II) complex, including the first evidence for a bound superoxo species, *Proc. Natl. Acad. Sci. U.S.A. 102*, 5340−5345.
29. Price, J. C., Barr, E. W., Glass, T. E., Krebs, C., and Bollinger, J. M., Jr. (2003) Evidence for Hydrogen Abstraction from C1 of Taurine by the High-Spin Fe(IV) Intermediate Detected during Oxygen Activation by Taurine:α-Ketoglutarate Dioxygenase (TauD), *J. Am. Chem. Soc. 125*, 13008−13009.

BI0526276